Available online at www.sciencedirect.com
ScienceDirect
Sensors and Actuators B 117 (2006) 480–487
SENSORS AND ACTUATORS B CHEMICAL
www.elsevier.com/locate/snb

Bioelectrocatalytic self-assembled thylakoids for micro-power and sensing applications

Kien B. Lam [a,b,*], Elizabeth F. Irwin [c], Kevin E. Healy [c,d], Liwei Lin [a,b]

[a] *Department of Mechanical Engineering, University of California at Berkeley, Berkeley, CA 94720, USA*
[b] *Berkeley Sensor and Actuator Center, University of California at Berkeley, Berkeley, CA 94720, USA*
[c] *Department of Bioengineering, University of California at Berkeley, Berkeley, CA 94720, USA*
[d] *Department of Materials Science and Engineering, University of California at Berkeley, Berkeley, CA 94720, USA*

Accepted 15 December 2005
Available online 18 May 2006

Abstract

Photosynthetic sub-cellular plant structures called thylakoid were immobilized onto a gold electrode surface that had been functionalized by bioelectrocatalytic self-assembled monolayers (bio-SAMs) of cystamine and pyrroloquinoline quinone (PQQ). The goal is to achieve direct transfer of electrons from thylakoids to the electrode via the bio-SAMs to increase the electrical efficiency of MEMS photosynthetic electrochemical cells (μPECs). The immobilization technique could also be used in MEMS bio-sensing and microbial fuel cell applications. Quartz crystal microbalance with dissipation (QCM-D) was used to characterize the deposition kinetics of cystamine, PQQ, and thylakoids. Using QCM-D, the surface coverage of these three layers was determined to be, respectively, 7.9×10^{-10} mol/cm^2, 3.3×10^{-10} mol/cm^2, and 1.5×10^6 thylakoids/cm^2. The cystamine and PQQ monolayers formed within 5 min, while the thylakoid layer required over 1 h. Each layer was shown to be covalently linked to the substrate or layer underneath and thus was able to survive repeated rinsing in water or buffer.

Keywords: Photosynthesis; Self-assembled monolayer (SAM); Thylakoid; Solar cell; Fuel cell

1. Introduction

Photosynthetic electrochemical cells (PECs) are electrochemical cells that harness biocatalysts like photosynthetic bacteria [1–3], sub-cellular plant organelles [4–6], or photosynthetic enzymes [7–9] to convert light energy and water into electrical power. We recently demonstrated MEMS PECs (μPECs) powered by live blue-green algae [10] and by sub-cellular organelles known as thylakoids [11,12]. The μPECs generated about 500 mV open circuit voltage and on the order of 1 μA/cm^2 closed-circuit current density, results that are comparable to many biological electrochemical cells yet not powerful enough for most practical applications [13]. We showed that the primary issues limiting μPEC electrical output were (1) the "slow" transport of diffusional biocatalysts and redox (electron) mediators used in the reaction mixtures in the anode chamber and (2) the sensitivity of the biocatalysts and mediators to oxidation by O_2.

To address these two issues, in this paper, we demonstrate immobilizing photosynthetic thylakoids directly onto a gold electrode surface by means of bioelectrocatalytic self-assembled monolayers (bio-SAMs). We then monitor the deposition kinetics of bio-SAM formation on the gold surface and thylakoid immobilization the bio-SAMs via a surface technique known as quartz crystal microbalance with dissipation (QCM-D). Thylakoid immobilization via bio-SAMs has not yet been demonstrated in the literature, and our supposition is that such a scheme would promote direct transfer of electrons from thylakoids to the electrode, thus enhancing electrical output.

This supposition is based on work by Katz et al., who isolated photosynthetic enzymes called reaction centers from photosynthetic bacteria and immobilized them onto a PtO electrode via bio-SAMs [14]. While this "photobioelectrode" was capable of converting light into electricity, it did not possess bio-sensing capabilities that we are proposing using bio-SAM-immobilized thylakoids. There has also been previous work

* Corresponding author. Tel.: +1 408 768 1287.
E-mail address: kblam@ocf.berkeley.edu (K.B. Lam).

0925-4005/$ – see front matter © 2006 Published by Elsevier B.V.
doi:10.1016/j.snb.2005.12.057

immobilizing thylakoids and other sub-cellular plant components onto electrodes by polymeric encapsulation [15–17] and chemical crosslinking [5]. Although such encapsulation methods increased the stability of the photosynthetic components, current densities were generally low at less than 1 $\mu A/cm^2$.

Willner and collaborators immobilized enzymes such as glucose oxidase and lactate dehydrogenase onto electrodes by means of various bio-SAMs for enzymatic fuel cell applications [13,18,19]. Using methods to be elaborated upon in Section 2, we shall adapt these aforementioned techniques to immobilize thylakoids on gold electrodes for μPEC and bio-sensing applications (which take advantage of the thylakoids' ability to detect herbicides and other environmental contaminants [5]).

2. Theory

MEMS-based photosynthetic electrochemical cells (μPECs), or bio-solar cells, harness photobiocatalysts like live photosynthetic bacteria [1–3], sub-cellular plant organelles [4–6], or photosynthetic enzymes [7–9] to convert light energy and water into electrical power. PECs are distinct from but related to bio-fuel cells that use biocatalysts ranging from microorganisms [20,21] to enzymes [22,23] to catabolize bio-substrates such as glucose into electricity. Previously, μPECs were demonstrated using live cultures of blue-green algae [10] or sub-cellular organelles known as thylakoids [11] as photobiocatalysts. These μPECs generated about 0.5 V open circuit voltage and on the order of 1 $\mu A/cm^2$ closed-circuit current density, results that are comparable to many biological electrochemical cells yet not powerful enough for most practical applications [13]. It was shown that the primary issues limiting the electrical output and efficiency of the μPECs were (1) the "slow" transport of diffusional photobiocatalysts and redox (electron) mediators in the reaction mixtures of the anode compartments and (2) the sensitivity of the photobiocatalysts and mediators to oxidation by O_2 [24].

One approach to address these two issues and thus increase efficiency is to functionalize the gold anode surface of the μPEC with photobiocatalysts (i.e. thylakoids) arranged in a so-called "bioelectrocatalytic self-assembled monolayer," or bio-SAM. As illustrated in Fig. 1, thylakoids are "chained" to the anode via linking molecules PQQ and cystamine. With photobiocatalysts directly immobilized on the anode (i.e. not in solution), it is proposed that electrons released from illuminated thylakoids are transferred directly to the anode—thus eliminating both the "slowness" of diffusional mediators and interference of electron transfer by O_2. In this paper, we demonstrate the synthesis of this thylakoids bio-SAM and characterize the synthesis using a surface measurement technique known as quartz crystal microbalance with dissipation (QCM-D).

There has been previous work immobilizing thylakoids and other sub-cellular plant components onto electrodes by polymeric encapsulation [15–17] and chemical crosslinking [5]. Although such encapsulation methods increased the stability of the photosynthetic components, current densities were generally low at less than 1 $\mu A/cm^2$. Katz linked photosynthetic enzymes onto a PtO electrode using bio-SAMs [7,14]. Willner and collaborators immobilized enzymes such as glucose oxidase and lactate dehydrogenase onto electrodes by means of various bio-SAMs for enzymatic fuel cell applications [13,18,19]. Using methods to be elaborated upon in Section 2, we shall adapt these aforementioned techniques to immobilize thylakoids on gold electrodes for μPEC and bio-sensing applications (which take advantage of the thylakoids' ability to detect herbicides and other environmental contaminants [5]) (Fig. 2).

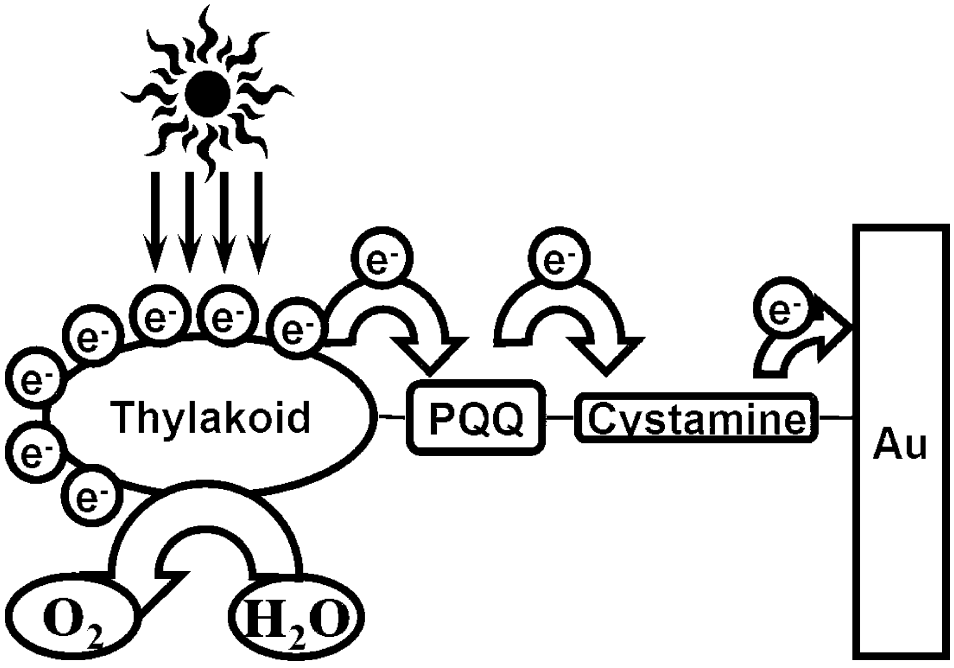

Fig. 1. Proposal to functionalize gold anode surface of MEMS photosynthetic electrochemical cell with photobiocatalysts arranged in bioelectrocatalytic self-assembled monolayers (bio-SAMs); illumination of thylakoids is expected to yield electrons that are transferred via the bio-SAMs to the gold anode surface.

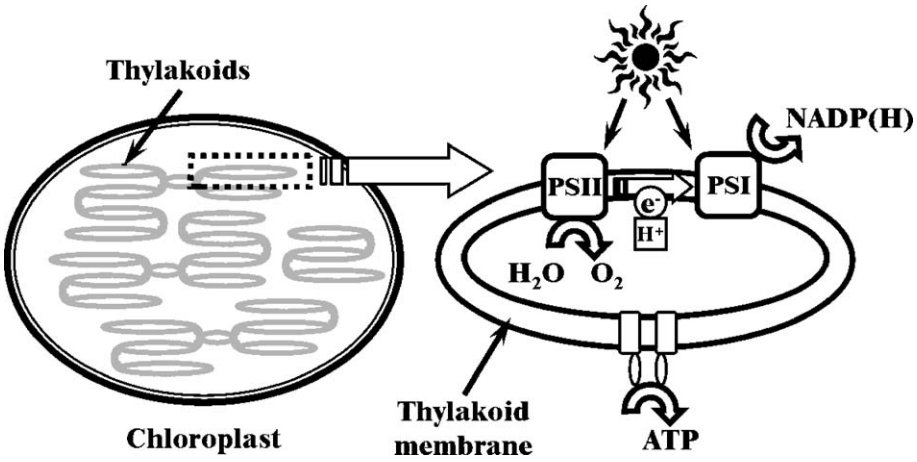

Fig. 2. (a) Chloroplast, a membrane-bound organelle inside plant cells that contain smaller membrane-bound structures called thylakoids. (b) Detail view of a thylakoid, which have photosynthetic enzymes embedded on the outer membrane.

3. Experiment

3.1. Synthesis of cystamine and PQQ bio-SAMs

We first created the Au substrates on which we would synthesize the bio-SAMs by thermally evaporating Cr/Au (500 Å/1500 Å thick) on a 4 in. Si wafer and dicing the wafer into 1 cm × 1 cm dice, which served as the Au substrates. Because bio-SAMs surface chemistry is highly sensitive to contamination, the Au substrates were then cleaned in a 5:1:1 solution of ultrapure water (UPW), ammonium hydroxide (NH_4OH), and hydrogen peroxide (H_2O_2) heated to 75 °C. Likewise, to prevent surface contamination, all glassware used in the synthesis of the bio-SAMs was first cleaned in Contrad solution, rinsed in ultrapure water, and bake-dried.

The chemical reactions of the bio-SAMs synthesis are illustrated in Fig. 3. All chemicals were purchased from Sigma–Aldrich and used as received. The Au substrate was first functionalized with a cystamine monolayer by soaking the Au substrate in 0.02 M cystamine for 2 h in a Petri dish (Fig. 3a). The substrate was then "rinsed" in UPW and HEPES buffer to remove physisorbed (i.e. not chemically linked) cystamine. This "rinsing" was done by aspirating the cystamine from the Petri dish and replacing it with UPW, in which the Au substrates soaked for 5 min; then the UPW was aspirated from the Petri dish and replaced with 0.01 M HEPES buffer (pH 7.5), in which the substrates soaked for another 5 min.

Next, pyrroloquinoline quinone (PQQ, Fig. 3f) was deposited on the cystamine monolayer using EDC to crosslink the carboxyl (–COOH) group of PQQ with the amino ($–NH_2$) group of cystamine to form an amide bond [25,26]. EDC is the acronym for the carbodiimide named *N*-(3-dimethyaminopropyl)-*N*′-ethylcarbodiimide; it is a zero-length crosslinking agent because, in forming the amide bond, it does not introduce additional chemical structure between the conjugating molecules [27]. EDC reacts with carboxyl groups to form highly reactive intermediates that then react with nucleophiles like amino groups, resulting in an amide bond. The specific steps of the PQQ deposition were as follows. After the substrate was rinsed with UPW and HEPES buffer following cystamine deposition, it was soaked in a solution of 3 mM PQQ and 10 mM EDC in HEPES buffer for 3 h; then the substrate was again "rinsed" in HEPES buffer to remove PQQ that was only physisorbed (as opposed to chemisorbed) onto the cystamine monolayer. The result was the cystamine–PQQ SAMs shown in Fig. 3c, providing the foundation on which thylakoids – the photobiocatalysts – will be immobilized.

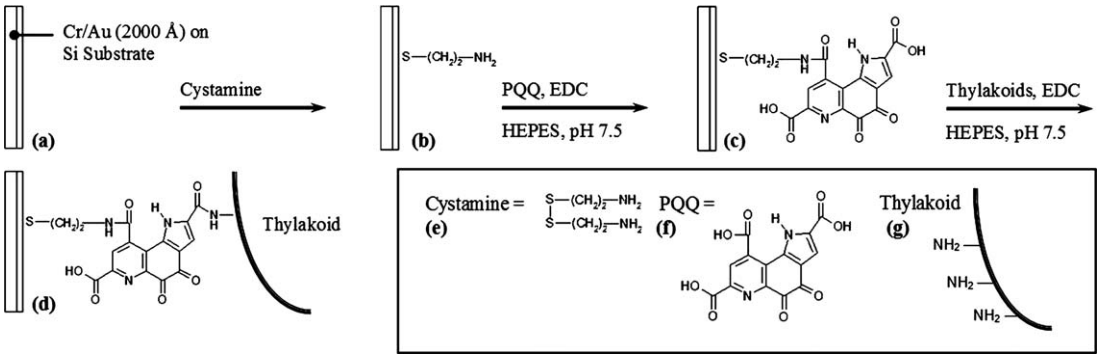

Fig. 3. Chemical reaction steps of synthesizing bioelectrocatalytic SAMs (cystamine and PQQ) on gold substrate and immobilizing thylakoids on SAMs.

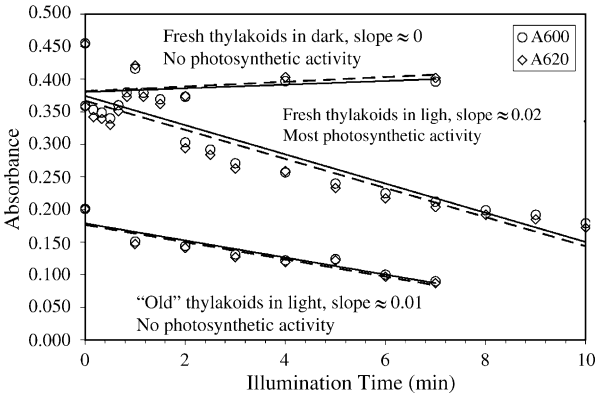

Fig. 4. Photosynthesis-driven reduction of electron mediator DCPIP by isolated thylakoids in a representative experiment: the absorbance of a solution containing thylakoids and DCPIP was measured using a spectrophotometer at two wavelengths. Fresh thylakoids in light yielded the greatest slope and, thus, greatest activity compared with 8-day-old thylakoids and thylakoids kept in the dark.

3.2. Preparation and immobilization of thylakoids

Thylakoids were then isolated from baby spinach purchased from the grocery store using a common fractionation procedure [28,29], yielding a thylakoid slurry with a chlorophyll concentration of 0.14 mg chlorophyll/mL. The light absorbance of the isolated thylakoids was measured spectrophotometrically using the artificial electron acceptor 2,6-dichloroindophenol (DCPIP) [28]. The results in Fig. 4 show that freshly isolated thylakoids under illumination exhibit the greatest photosynthetic activity (i.e. steepest slope) compared with thylakoids in the dark or "old" thylakoids. From the absorbance data, the specific activity of the thylakoid preparation was then determined to be 0.44 μmol DCPIP reduced/mg chlorophyll/min [28].

After determining that the isolated thylakoids were photosynthetically active, we proceeded with immobilizing the thylakoids onto the cystamine and PQQ bio-SAMs. We postulated that we could covalently link the amino groups (–NH_2) on the thylakoid membrane to the carboxyl groups (–COOH) of the PQQ monolayer – thus forming an amide bond – just like we had linked the carboxyl groups of PQQ to the amino groups of cystamine. The process is represented in Fig. 3 d and preceded as follows. After cystamine and PQQ were immobilized on the Au substrate (Fig. 3b and c), the substrates had been rinsed and kept in 0.01 M HEPES buffer (pH 7.5). This HEPES buffer was aspirated, and the substrates were put in a 10 mL solution of 10 mM EDC in HEPES buffer. Then 2 mL of the thylakoid preparation was added to the solution, and the substrates were allowed to soak for 3 h, shielded from light (i.e. kept in the dark). The substrates were then rinsed and stored in HEPES and shielded from light until used. The result was the thylakoids-based bio-SAM structure illustrated in Fig. 3d.

3.3. Characterization of synthesis of bio-SAMs

We then characterized the deposition kinetics of cystamine, PQQ, and thylakoids using the QCM-D surface chemistry technique. QCM-D is a sensitive mass sensor in which an ac voltage is pulsed across a piezoelectric quartz crystal at the crystal's resonant frequency (5 MHz) and at several overtones ($n = 3, 5, 7$, corresponding to 15, 25, 75 MHz) [30–32]. The pulses cause the crystal to oscillate in shear mode at each frequency. The shear wave at each frequency is then allowed to dampen, providing viscoelastic information about a film adsorbed to the crystal. In our experiments, we used the Q-Sense D300 QCM-D system, which is sensitive to surface coverage as low as 0.18 ng/cm^2 [30]. For the special case of thin, rigid films, the Sauerbrey equation relates the change in the resonant or overtone frequency of the crystal, Δf, with the change in mass per unit area, Δm, of the film adsorbed to the crystal surface, including bound water [30,31]:

$$\Delta m = \frac{C}{n}\Delta f$$

where Δm is in units of ng/cm^2, C a constant that depends on the physical properties of the crystal ($C = 17.7$ ng/cm^2/Hz for the quartz crystal in our case [30]), and n is the overtone number (=1, 3, 5, 7, . . .). Then the surface coverage film could be calculated as

$$\Gamma = \frac{\Delta m}{\mathrm{FW}}$$

where Γ is in units of mol/cm^2 and FW is the formula weight of the adsorbed species. For the QCM-D measurements, the cystamine, PQQ, and thylakoids were deposited in the QCM-D reaction chamber onto custom Q-Sense gold-covered crystals rather than on Si/Au substrates using a procedure similar to that described above.

4. Results and discussion

The QCM-D monitored in real-time the frequency change (i.e. decreasing Δf) of the crystal as material (cystamine, PQQ, thylakoids) was being introduced into the QCM-D reaction chamber and adsorbed to the surface (increasing Δm). Fig. 5 plots the change in frequency normalized by the overtone, $\Delta f/n$. However, because Δf is noisy at the resonant frequency ($n = 1$), we have shown $\Delta f/n$ only for overtones $n = 3$, 5 and 7.

Fig. 5a shows the kinetics of the adsorption of cystamine to the Au surface and subsequent linking of PQQ to cystamine. Ultrapure water first was introduced into the QCM-D chamber to equilibrate with the reaction chamber, generating no deposition onto the surface as shown ($\Delta f/n \approx 0$). But upon introducing cystamine, normalized change in frequency $\Delta f/n$ decreased to the range of −8 to −9.5 Hz (depending on the overtone) within 5 min and remained there for the 2 h allotted for cystamine deposition. The speed with which the cystamine covered the surface (within 5 min) indicated that we could dramatically reduce the 2 h cystamine reaction time.

After the cystamine reaction, UPW was introduced to "rinse" physisorbed (i.e. not chemisorbed) cystamine from the Au surface, with the result that $\Delta f/n$ increased to the range of −6.8 to −7.0 Hz (i.e. mass rinsed off of surface). Using the Sauerbrey relation and cystamine FW = 152.27 g/mol, the surface coverage of the cystamine monolayer (including bound water) on the Au

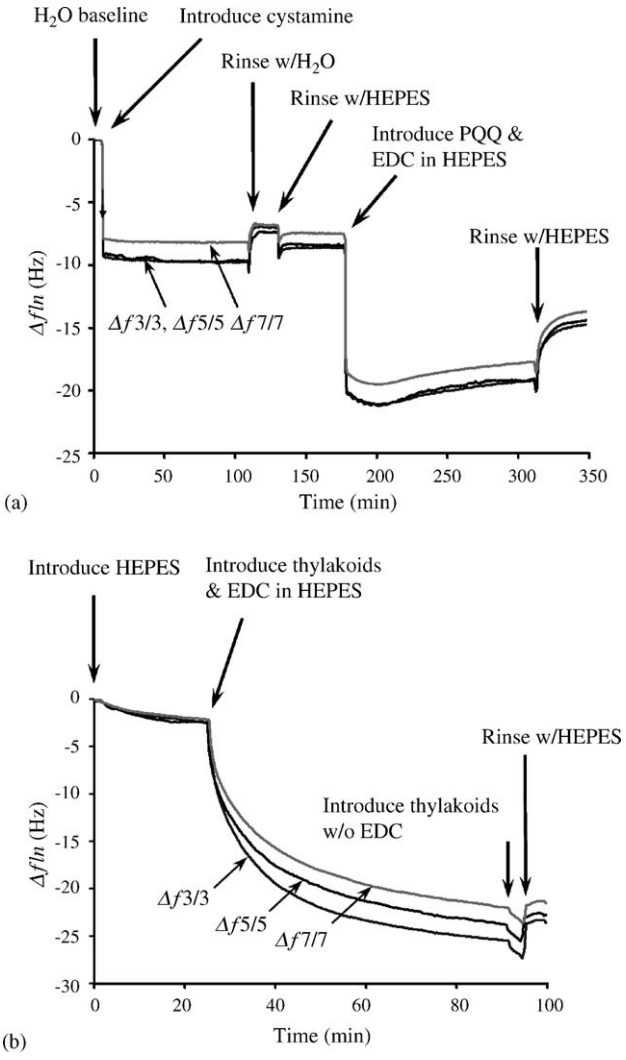

Fig. 5. QCM-D characterization of deposition kinetics of (a) cystamine and PQQ monolayers onto Au surface and (b) thylakoids onto cystamine–PQQ monolayers. Normalized changes in frequency, $\Delta f/n$, of QCM-D crystal for several overtones (15, 25, 74 MHz) are used with the Sauerbrey relationship to calculate surface coverage of deposited layers.

surface was determined in terms of mass Δm and in terms of moles Γ:

$$\Delta m_{\text{cystamine}} = C\frac{\Delta f}{n} = (17.7\,\text{ng/cm}^2/\text{Hz})(6.8\,\text{Hz}) = 120\,\text{ng/cm}^2,$$

$$\Gamma_{\text{cystamine}} = \frac{\Delta m}{\text{FW}} = 7.9\times10^{-10}\,\text{mol/cm}^2$$

The surface coverage in terms of number density of cystamine molecules was then also calculated

$$\Gamma'_{\text{cystamine}} = (6.022\times10^{23})\Gamma_{\text{cystamine}} = 4.8\times10^{14}\,\text{cm}^{-2}$$

This cystamine surface coverage, $\Gamma = 7.9\times10^{-10}\,\text{mol/cm}^2$, lying in the range of 10^{-9} to $10^{-10}\,\text{mol/cm}^2$, corresponded to that of the classic self-assembled monolayers [33]. To see that this is so, we do a back-of-the-envelope calculation in which we model a representative molecule as a sphere of diameter 10 Å = 1 nm. If such spherical molecules were self-assembled into a square lattice on the surface, then in an area of $1\,\text{cm}\times1\,\text{cm} = 10^7\,\text{nm}\times10^7\,\text{nm}$, there would be $10^7\times10^7 = 10^{14}\,\text{molecules/cm}^2$. Since the cystamine surface number density was $4.8\times10^{14}\,\text{molecules/cm}^2$, we are justified in our use so far of the terms "monolayer" and "SAM" when referring to the cystamine layer on the Au surface.

HEPES buffer was next introduced into the QCM-D chamber, resulting in a $\Delta f/n$ drop to the range of −7.5 to −8.6 Hz. Then PQQ and the EDC crosslinker in HEPES buffer were introduced, causing a decrease in $\Delta f/n$ to −19.2 to −20.8 Hz within 10 min and settling at −17.7 to −19.2 Hz after 2.5 h. Because of the speed with which PQQ formed the monolayer, we could elect to shorten the PQQ reaction time. After rinsing away physisorbed PQQ with HEPES, $\Delta f/n$ rose to −13.7 to −14.8 Hz (material rinsed away). Using the $\Delta f/n$ of −7.5 to −8.6 Hz from the first HEPES rinse as baseline, this corresponded to a net $\Delta f/n$ for the PQQ deposition of −6.2 Hz. Using the Sauerbrey relation and PQQ FW = 330.21 g/mol, the surface coverage of the PQQ monolayer (including bound water) was calculated again in terms of mass Δm and moles Γ:

$$\Delta m_{\text{PQQ}} = C\frac{\Delta f}{n} = (17.7\,\text{ng/cm}^2/\text{Hz})(6.2\,\text{Hz}) = 110\,\text{ng/cm}^2,$$

$$\Gamma_{\text{PQQ}} = \frac{\Delta m}{\text{FW}} = 3.3\times10^{-10}\,\text{mol/cm}^2$$

For reference, the surface coverage in terms of number density of PQQ molecules was then calculated

$$\Gamma'_{\text{PQQ}} = (6.022\times10^{23})\Gamma_{\text{PQQ}} = 2.0\times10^{14}\,\text{cm}^{-2}$$

Because the PQQ surface coverage was in the range of 10^{-9} to $10^{-10}\,\text{mol/cm}^2$ (or about $10^{14}\,\text{molecules/cm}^2$) characteristic of SAMs [33], we are again justified in calling the PQQ layer a SAM. We note that Katz had used cyclic voltammetry to deduce a PQQ surface coverage of $(1.0\pm0.1)\times10^{-10}\,\text{mol/cm}^2$ [26,34], a value that is less precise than the present QCM-D-measurement. Finally, we observe that the mass surface coverage of cystamine and PQQ were within 10% of each other ($\Delta m_{\text{cystamine}} = 120\,\text{ng/cm}^2$, $\Delta m_{\text{PQQ}} = 110\,\text{ng/cm}^2$). But because cystamine is less than half the molecular weight of PQQ ($\text{FW}_{\text{cystamine}} = 152.27$ g/mol, $\text{FW}_{\text{PQQ}} = 330.21$ g/mol) – and, thus, likely less than half the size – the molar surface coverage of cystamine was actually over twice that of PQQ ($\Gamma_{\text{cystamine}} = 7.9\times10^{-10}\,\text{mol/cm}^2$, $\Gamma_{\text{PQQ}} = 3.3\times10^{-10}\,\text{mol/cm}^2$).

Unlike cystamine and PQQ, thylakoids are not molecules but instead are sub-cellular plant organelles; nonetheless, we could still monitor thylakoid deposition onto the underlying cystamine–PQQ monolayers using QCM-D. The immobilization of thylakoids did not immediately follow the deposition of cystamine and PQQ; so in between the two QCM-D sessions, the crystal was removed from the QCM-D and stored in HEPES buffer. Upon re-installing the crystal back into the QCM-D, HEPES buffer was first introduced into the reaction chamber, again to equilibrate with the chamber. Fig. 5b shows the deposition kinetics. Apparently, some molecular components of

HEPES physisorbed to the surface, causing $\Delta f/n$ to decrease to the range of −2.1 to −2.4 Hz.

Then, by introducing thylakoids with the crosslinker EDC in HEPES buffer, the thylakoids were immobilized onto the existing PQQ monolayer over about 1 h, at which time $\Delta f/n$ declined to the range of −22.0 to −25.4 Hz. Unlike the cystamine and PQQ depositions, the thylakoids did not chemisorb within 5–10 min. But after about 1 h, it appeared as if the $\Delta f/n$ curve (being viewed in real-time) was showing asymptotic behavior, so we judged that the deposition time was sufficient. For thylakoid immobilization on the Si/Au substrates, we had allowed the full 3 h deposition time as reported in the procedure above. When thylakoids in HEPES buffer without the EDC crosslinker were then introduced, there was again another decline in $\Delta f/n$. But these thylakoids were just physisorbed to the surface because, when HEPES buffer was again introduced to rinse away physisorbed material, $\Delta f/n$ once again climbed back up—to −21.5 to −23.5 Hz. Thus, as we had proposed, the thylakoids with EDC did indeed chemisorb (i.e. bond covalently) to the PQQ monolayer; yet without EDC thylakoids only physisorbed. Using $\Delta f/n$ from the first HEPES rinsing as baseline (−2.1 to −2.4 Hz), the net change in $\Delta f/n$ due to thylakoid immobilization was therefore −19.4 to −21.1 Hz. Using the Sauerbrey relation, the surface coverage of thylakoids in terms of mass was

$$\Delta m_{\text{thylakoid}} = C\frac{\Delta f}{n} = (17.7\ \text{ng/cm}^2/\text{Hz})(19.4\ \text{Hz}) = 340\ \text{ng/cm}^2$$

Because thylakoids are not molecules, we did not calculate the surface coverage in terms of moles as we did for cystamine and PQQ. However, we could estimate the number density of thylakoids on the surface (i.e. number of thylakoids per square area). Thylakoids are flattened membrane-bound sacs on the order of 1 μm in diameter. If we model a typical thylakoid as a flat cylindrical disc of diameter $d = 1$ μm and thickness, say, $t = 0.25$ μm, then the model thylakoid would have volume:

$$V_{\text{thylakoid}} \approx \pi\frac{d^2}{4}t = 0.196\ \mu\text{m}^3 = 1.96 \times 10^{-13}\ \text{cm}^3$$

Thylakoids consist of primarily of water and proteins, which have densities of 1.0 and 1.4 g/cm^3 [31], respectively; we took an average and assumed that thylakoids have a density of $\rho_{\text{thylakoid}} = 1.2$ g/cm^3. Then the number density of thylakoids could be estimated as

$$\Gamma'_{\text{thylakoid}} \approx \frac{\Delta m_{\text{thylakoid}}}{\rho_{\text{thylakoid}} V_{\text{thylakoid}}} = 1.46 \times 10^6\ \text{cm}^{-2}$$

We observe that the mass surface coverage of thylakoids ($\Delta m_{\text{thylakoids}} = 340$ ng/cm^2) was only about three times that of cystamine ($\Delta m_{\text{cystamine}} = 120$ ng/cm^2) and PQQ ($\Delta m_{\text{PQQ}} = 110$ ng/cm^2). By modeling a thylakoid as a flat disc of diameter 1 μm, an area of 1 cm × 1 cm = 10^4 μm × 10^4 μm would have $10^4 \times 10^4 = 10^8$ thylakoids/cm^2 in a packed monolayer. Yet, the number density surface coverage of thylakoids was only ∼10^6 thylakoids/cm^2, which was about 100 times less dense than an expected thylakoid monolayer would be.

A possible reason for the sub-monolayer surface density of the immobilized thylakoids could be that 1 h was not sufficient thylakoid deposition time in the QCM-D, even though 3 h were allowed for thylakoid deposition onto the Si/Au substrates. Yet, in Fig. 5, thylakoid deposition in the QCM-D seemed to exhibit asymptotic behavior after about 1 h. Another possible reason could be that the concentration of EDC was not high enough to crosslink enough of the available thylakoids to the underlying PQQ SAM. However, this was unlikely the case because an EDC concentration of 10 mM in the 2 mL QCM-D reaction chamber meant that the number of EDC molecules available for crosslinking thylakoids to the underlying PQQ SAM was (0.01 mol/L)(0.002 L)(6.022×10^{23} molecules/mol) = 1.2×10^{19} EDC molecules—many orders of magnitude greater than the number of thylakoids ultimately immobilized (∼10^6 thylakoids/cm^2). Yet another possible reason for the less-than-monolayer density of the immobilized thylakoids could be that an insufficient number of thylakoids (2 mL of 0.14 mg chl/mL preparation) was introduced to the QCM-D crystal surface. To remedy this, additional doses of thylakoids with EDC in HEPES buffer could be introduced after the initial dose.

Finally, we note that thylakoids have both carboxyl and amino groups on their membrane surfaces, so EDC could potentially crosslink these groups together in addition to crosslinking the thylakoids to PQQ; this could possibly disrupt electron transport along the membrane-bound enzyme complexes of the photosystems and thereby "de-activate" thylakoid activity. We thus needed to establish that EDC does not interfere with thylakoid activity. To do this, the solution of isolated thylakoids and EDC in HEPES previously described was prepared and allowed to react for 3 h, shielded from light. Electron mediator DCPIP was then added to the solution, and the absorbance of the solution was measured spectrophotometrically [24]. If the EDC did indeed "de-activate" the photosynthetic activity of the isolated thylakoids, then the thylakoids would not be able to reduce the DCPIP. DCPIP is blue in its oxidized form and colorless in its reduced form, so if DCPIP is not reduced,

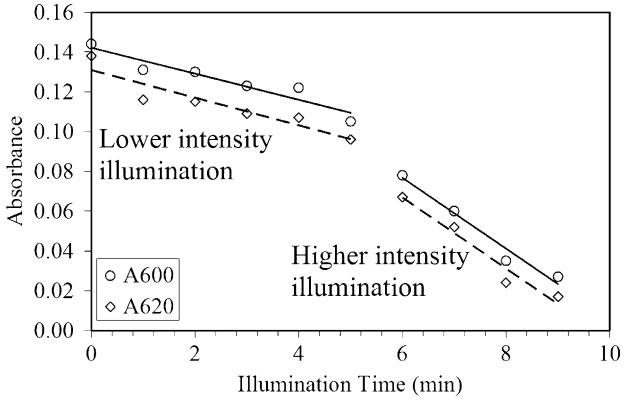

Fig. 6. Photosynthetic reduction of electron mediator DCPIP by isolated thylakoids that have been reacted with carbodiimide EDC crosslinker. Because of decrease in absorption, EDC did not "de-activate" thylakoid activity. DCPIP reduction was faster under higher intensity light (steeper slope) than normal intensity light.

then the absorbance of the solution would not decrease over time.

Yet, as shown in Fig. 6, because the absorbance of a thylakoid preparation with EDC present exhibited a decreasing downward slope, EDC did not appear to have "de-activated" thylakoid photosynthetic activity. The absorbance was measured spectrophotometrically at two wavelengths, 600 and 620 nm, and under two illumination intensities (not specified). We therefore surmise that thylakoids immobilized onto the PQQ monolayer by the action of EDC would likewise remain photosynthetically active.

5. Conclusion

We have successfully functionalized a gold electrode surface with a cystamine monolayer, onto which we covalently linked a monolayer of the redox mediator PQQ. We subsequently isolated thylakoids from baby spinach and immobilized them onto the cystamine–PQQ bio-SAMs. Using QCM-D, we characterized the formation of the cystamine–PQQ–thylakoids layers and verified that cystamine and PQQ indeed formed SAMs whereas thylakoids formed in sub-monolayer surface densities. We also established that the isolated thylakoids were not photosynthetically "de-activated" by the EDC crosslinker and, therefore, should also be active after immobilization.

The next steps entail electrochemically verifying that direct electron transfer from thylakoids via the bio-SAMs to the gold electrode surface is being achieved. This thylakoid immobilization scheme could potentially increase the current densities of MEMS photosynthetic fuel cells two orders of magnitude to hundreds of $\mu A/cm^2$. The scheme could also easily be extended to MEMS bio-sensing applications utilizing immobilized thylakoids to detect herbicides and various environmental pollutants. Finally, the immobilization chemistry developed in this paper could be applied to immobilizing other membrane-bound cellular or sub-cellular structures—such as unicellular microorganisms for MEMS microbial fuel cells [35].

Acknowledgments

This work was supported in part by an NSF grant (ECS-0300542), a DARPA/MTO/BioFlips grant (F30602-00-2-0566), and an ITRI fellowship.

References

[1] K. Tanaka, N. Kashiwagi, T. Ogawa, Effects of light on the electrical output of bioelectrochemical fuel-cells containing *Anabaena variabilis* M-2 mechanisms of the post-illumination burst, J. Chem. Technol. Biotechnol. 42 (1988) 235–240.

[2] T. Yagishita, S. Sawayama, K.-I. Tsukahara, T. Ogi, Effects of glucose addition and light on current outputs in photosynthetic electrochemical cells using *Synechocystis* sp. PCC6714, J. Biosci. Bioeng. 99 (1999) 210–214.

[3] S. Tsujimura, A. Wadano, K. Kano, T. Ikeda, Photosynthetic bioelectrochemical cell utilizing cyanobacteria and water-generating oxidase, Enzyme Microb. Technol. 29 (2001) 225–231.

[4] W. Haehnel, A. Heupel, D. Hengstermann, Investigations on a galvanic cell driven by photosynthetic electron transport, Z. Naturforsch. C: J. Biosci. 33 (1978) 392–401.

[5] D. Laberge, R. Rouillon, R. Carpentier, Comparative study of thylakoid membranes sensitivity for herbicide detection after physical or chemical immobilization, Enzyme Microb. Technol. 26 (2000) 332–336.

[6] M.J. Allen, A.E. Crane, Null potential voltammetry—an approach to the study of plant photosystem, Bioelectrochem. Bioenergy 3 (1976) 84–91.

[7] E.Y. Katz, A.A. Solovev, Photobioelectrodes on the basis of photosynthetic reaction centers. Study of exogenous quinines as possible electron transfer mediators, Anal. Chim. Acta 266 (1992) 97–106.

[8] L.A. Drachev, A.A. Jasaitis, A.D. Kaulen, A.A. Kondrashin, L.V. Chu, A.Y. Semenov, I.I. Severina, V.P. Skulachev, Reconstitution of biological molecular generators of electric current: cytochrome oxidase, J. Biol. Chem. 251 (1976) 7072–7076.

[9] A.F. Janzen, Photoelectrochemical conversion using reaction-centre electrodes, Nature 286 (1980) 584–585.

[10] H.P. Bennetto, Electricity generation by microorganisms, Biotechnol. Educ. 1 (1990) 163–169.

[11] D.H. Park, J.G. Zeikus, Electricity generation in microbial fuel cells using neutral red as an electronophore, Appl. Environ. Microbiol. 66 (2000) 1292–1297.

[12] A. Halme, X. Zhang, A. Ranta, Study of biological fuel cells, in: Proceedings of the Second Annual Advances in R&D: The Commercialization of Small Fuel Cells and Battery Technologies for Use in Portable Applications, New Orleans, USA, 2000.

[13] H.-H. Kim, N. Mano, Y. Zhang, A. Heller, Miniature membrane-less biofuel cell operating under physiological conditions at 0.5 V, J. Electrochem. Soc. 150 (2003) A209–A213.

[14] K.B. Lam, M. Chiao, L. Lin, A micro photosynthetic electrochemical cell, in: Proceedings of the IEEE Conference on Micro Electro Mechanical System, MEMS 2003, Kyoto, Japan, 2003.

[15] K.B. Lam, E. Johnson, L. Lin, A bio-solar cell powered by sub-cellular plant photosystems, in: Proceedings of the IEEE Conference on Micro Electro Mechanical System, MEMS 2004, Maastricht, The Netherlands, 2004.

[16] E. Katz, A.N. Shipway, I. Willner, Biochemical fuel cells, in: W. Vielstich, A. Lamm, H.A. Gasteiger (Eds.), Handbook of Fuel Cells—Fundamentals, Technology and Applications, vols. 355–381, John Wiley & Sons, Chichester, West Sussex, 2003.

[17] K.B. Lam, MEMS microbial fuel cells and photosynthetic electrochemical cells, PhD Dissertation, Mech. Eng., University of California at Berkeley, Berkeley, CA, 2005.

[18] H. Ochiai, H. Shibata, Y. Sawa, T. Katoh, Properties of the chloroplast film electrode immobilized on an SnO_2-coated glass plate, Photochem. Photobiol. 35 (1982) 149–155.

[19] R Rouillon, N. Boucher, Y. Gingras, R. Carpentier, Potential for the use of photosystetn II submembrane fractions immobilized in poly(vinyalcohol) to detect heavy metals in solution or in sewage sludge, J. Chem. Technol. Biotechnol. 75 (2000) 1003–1007.

[20] R. Carpentier, S. Lemieux, M. Mimeault, M. Purcell, D.C. Goetze, A photoelectrochemical cell using immobilized photosynthetic membranes, J. Electroanal. Chem. 276 (1989) 391–401.

[21] E.Y. Katz, A.Y. Shkuropatov, V.A. Shuvalov, Electrochemical approach to the development of a photoelectrode on the basis of photosynthetic reaction centers, Bioelectrochem. Bioenergy 23 (1990) 239–247.

[22] E. Katz, A. Ricklin, V. Heleg-Shabtai, I. Willner, A.F. Buckmann, Glucose oxidase electrodes via reconstitution of the apo-enzyme: tailoring of novel glucose biosensors, Anal. Chim. Acta 385 (1999) 45–58.

[23] A. Bardea, E. Katz, A.F. Buckmann, I. Willner, NAD+-dependent enzyme electrodes: electrical contact of cofactor-dependent enzymes and electrodes, J. Am. Chem. Soc 119 (1997) 9114–9119.

[24] D. Voet, J.G. Voet, Biochemistry, 2nd ed., John Wiley & Sons Ltd., New York, NY, 1995.

[25] E. Katz, D.D. Schelerth, H.L. Schmidt, Electrochemical study of pyrroloquinoline quinine covalently immobilized as a monolayer onto cystamine-modified gold electrode, J. Electroanal. Chem. 367 (1994) 59–70.

[26] E. Katz, T. Lotzbeyer, D.D. Schlereth, W. Schuhmann, H.L. Schmidt, Electrocatalytic oxidation of reduced nicotinamide coenzymes at gold and platinum electrode surfaces modified with a monolayer of pyrrolo-

quinoline quinine-effect of Ca^{2+} cations, J. Electroanal. Chem. 373 (1994) 189–200.
[27] G.T. Hermanson, Bioconjugate Techniques, Academic Press, San Diego, 1996.
[28] S.P. Berg, Plant Physiology: Photosynthesis Laboratory Protocol, Minnesota State University at Winona (Winona State University), Winona, 2004.
[29] A. Melis, Plant and Microbial Biology 135: Physiology and Biochemistry of Plants Laboratory Manual, University of California at Berkeley, Berkeley, CA, 2003.
[30] Q-Sense, QCM-D Technology, 2004. http://www.q-sense.com/.
[31] F. Hook, C. Larsson, C. Fant, Biofunctional surfaces studied by quartz crystal microbalance with dissipation monitoring, in: Encyclopedia of Surface and Colloid Science, Marcel Dekker, 2002, pp.774–791.
[32] M. Rodahl, B. Kasemo, A simple setup to simultaneously measure the resonant frequency and absolute dissipation factor of a quartz crystal microbalance, Rev. Sci. Instrum. 67 (1996) 3238–3241.
[33] K.L. Prime, G.M. Whitesides, Self-assembled organic monolayers: model systems for studying adsorption of proteins at surfaces, Science 252 (1991) 1164–1167.
[34] E. Katz, D.D. Schlereth, H.L. Schmidt, Reconstitution of the quinoprotein glucose dehydrogenase from its apoenzyme on a gold electrode modified with a monolayer of pyrroloquinoline quinine, J. Electroanal. Chem. 368 (1994) 165–171.
[35] M. Chiao, K.B. Lam, L. Lin, A microfabricated microbial fuel cell, in: Proceedings of the IEEE Conference on Micro Electro Mechanical System, MEMS 2003, Kyoto, Japan, 2003.

Biographies

Kien Bang Lam received the BS degree in mechanical engineering at the University of California at Berkeley in 1997, the MS degree in mechanical engineering at the University of Michigan at Ann Arbor in 1999, and the PhD in mechanical engineering at the University of California at Berkeley in 2005. He is currently a senior process engineer at Intel Corporation in Santa Clara, CA. Previously, he was a mechanical engineer at Applied Materials in Santa Clara, CA, from 1999 to 2001; an intern researcher at Ford Research Laboratory from 1998 to 1999; a graduate student researcher in the Mechanical Engineering Department at the University of Michigan at Ann Arbor from 1997 to 1999; an intern at Lawrence Berkeley National Laboratory from 1996 to 1997.

Kevin E. Healy is a professor at the University of California at Berkeley in the Departments of Bioengineering and Materials Science and Engineering. He received a bachelor of science degree from the University of Rochester in chemical engineering in 1983. In 1985 he received a masters of science degree in bioengineering from the University of Pennsylvania, and in 1990 he received a PhD in bioengineering also from the University of Pennsylvania. He was elected a fellow of the American Institute of Medical and Biological Engineering in 2001. He has authored or co-authored more than 150 published articles, abstracts, or book chapters which emphasize the relationship between materials and the tissues they contact. His research interests include the design and synthesis of biomimetic materials that actively direct the behavior of mammalian cells to facilitate regeneration of tissues and organs. Major discoveries from his laboratory have centered on the control of cell behavior and tissue formation in contract with surfaces either modified with peptides or spatially distributed chemistry that induces cell differentiation. These materials find applications in medicine, dentistry, and biotechnology. He is currently an assistant editor of the Journal of Biomedical Materials Research. He has served on numerous panels and grant review study sections for NIH. He has given more than 100 invited lectures in the fields of biomedical engineering and biomaterials. He is a named inventor on four issued United States Patents relating to biomaterials, and has founded BioEngineered Materials Inc., a corporation founded to develop materials for applications in biotechnology and medicine, and Cardiomimetix Inc., a new company focused on intravascular devices and cardiac tissue engineering.

Liwei Lin received his BS degree from National Tsing-Hua University, Taiwan in 1986 and the MS and PhD degrees in mechanical engineering from the University of California, Berkeley, in 1991 and 1993, respectively. He joined BEI Electronics Inc., USA, from 1993 to 1994 in microsensors research and development. He was an associate professor in the Institute of Applied Mechanics, National Taiwan University, Taiwan, from 1994 to 1996 and an assistant professor at the Mechanical Engineering Department at the University of Michigan from 1996 to 1999. He joined the University of California at Berkeley in 1999 and is now a professor at Mechanical Engineering Department and co-director at Berkeley Sensor and Actuator Center, NSF/Industry/University Research Cooperative Center. His research interests are in design, modeling and fabrication of micro/nano structures, micro/nano sensors and micro/nano actuators as well as mechanical issues in micro/nano electromechanical systems and he holds eight U.S. patents. Dr. Lin is the recipient of the 1998 NSF CAREER Award for research in MEMS Packaging and the 1999 ASME Journal of Heat Transfer best paper award for his work on micro scale bubble formation. He is a subject editor for IEEE/ASME Journal of Microelectromechanical Systems and North and South America Editor for Sensors and Actuators – A Physical. He has been the founding chairman of the ASME MEMS division since 2004.